

Vacuum-processable ladder-type oligophenylenes for organic–inorganic hybrid structures: synthesis, optical and electrochemical properties upon increasing planarization as well as thin film growth

Björn Kobin,^a Lutz Grubert,^a Sylke Blumstengel,^{*b} Fritz Henneberger^{*b} and Stefan Hecht^{*a}

Received 14th November 2011, Accepted 12th December 2011

DOI: 10.1039/c2jm15868j

A novel synthetic route to even-numbered ladder-type oligo(*p*-phenylene)s (LOPPs) carrying no solubilizing groups to facilitate vacuum-processing is presented. The influence of increasing bridging adjacent phenylene units on the optical and electrochemical properties is discussed in the series of *p*-sexiphenyl **6P**, terfluorene **3F**, and ladder-type sexiphenyl **L6P**. The influence of the extension of the π -system is taken into consideration as well. Furthermore it is shown that highly ordered thin films of **L6P** on alumina surfaces can be prepared by organic molecular beam deposition (OMBD).

1. Introduction

Optoelectronic devices incorporating organic semiconducting materials are heavily investigated to achieve higher device efficiencies and longer durability in combination with their light weight, flexibility, and potentially low cost.¹ The integration of organic and inorganic semiconductor materials to unite specific favorable properties of both material classes is particularly promising. To achieve proper interaction of both semiconductor materials in order to promote either energy or electron transfer between the two device components, the energy level alignment at the interface and hence the organization of the molecular building blocks is crucial.² In order to gain a detailed understanding of these important processes it is essential to construct well-defined inorganic–organic hybrid structures. Such model systems can be realized by thin-film growth of organic molecules on semiconductor surfaces by vapor deposition or molecular beam deposition techniques.³ The most important prerequisites for the molecular building blocks to be employed are therefore their thermal stability beyond the evaporation temperatures. Clearly, the organic material should possess the desired optoelectronic properties, such as high absorption coefficients and luminescence efficiencies, narrow absorption and luminescence bands as well as a small Stokes shift to enable efficient exciton migration within the organic layer. Furthermore, the organic component should resist any type of optically or electrochemically induced degradation.

One of the prime organic semiconductors, meeting many but not all of the aforementioned conditions, is *p*-sexiphenyl **6P**—the

“fruitfly” of organic electronics. Besides studies on the application in organic light-emitting diodes (OLEDs)^{4,5} there are many reports about its crystallographic structures on a variety of metallic and dielectric surfaces,⁶ notably also on the electronic structure at the interface with ZnO.² Furthermore, non-radiative energy transfer between ZnO and a spiro-derivative of **6P** has been demonstrated.⁷ However, due to its intrinsic flexibility, in particular its rotational degrees of freedom along the aryl–aryl connections, oligo- and poly(*p*-phenylene)s in general display rather broad absorption and emission spectra and a significant Stokes shift. To overcome these restrictions, we focused on bridged oligo(*p*-phenylene)s, so-called ladder oligo(*p*-phenylene)s (LOPPs), which due to their fixed planar geometry should exhibit the desired optical features. Note that to date a large number of typically odd-numbered oligomers as well as polymers of that type has been synthesized and studies of their optical and electronic properties as well as their applicability in OLEDs, photovoltaic cells, and electronic materials have been described in the literature,⁸ yet all these examples necessitate long alkyl chains to provide sufficient solubility for solution processing. However, the significant weight bestowed by the side chains prohibits their evaporation without thermal degradation and therefore it is not surprising that thus far there is no report on vacuum-processable LOPPs.⁹ Furthermore, note that even-numbered oligomers have been synthesized only up to four phenylene units. Herein, we disclose a new synthetic route to even-numbered LOPPs, designed specifically for vacuum-based deposition techniques. We describe both the synthesis and characterization with regard to their optical and electrochemical properties in solution as well as the growth of thin films on alumina surfaces by organic molecular beam deposition (OMBD). These molecules should enable the realization of the targeted organic–inorganic semiconductor hybrid structures to allow for efficient exciton and charge transfer across the organic–inorganic interface.

^aDepartment of Chemistry, Humboldt-Universität zu Berlin, Brook-Taylor-Str. 2, 12489 Berlin, Germany. E-mail: sh@chemie.hu-berlin.de

^bInstitut für Physik, Humboldt-Universität zu Berlin, Newtonstrasse 15, 12489 Berlin, Germany. E-mail: sylke.blumstengel@physik.hu-berlin.de; fh@physik.hu-berlin.de

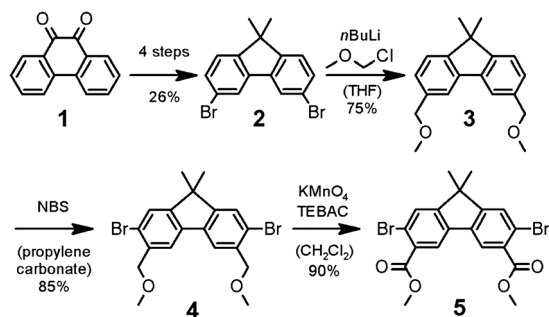
2. Results and discussion

2.1 Synthesis

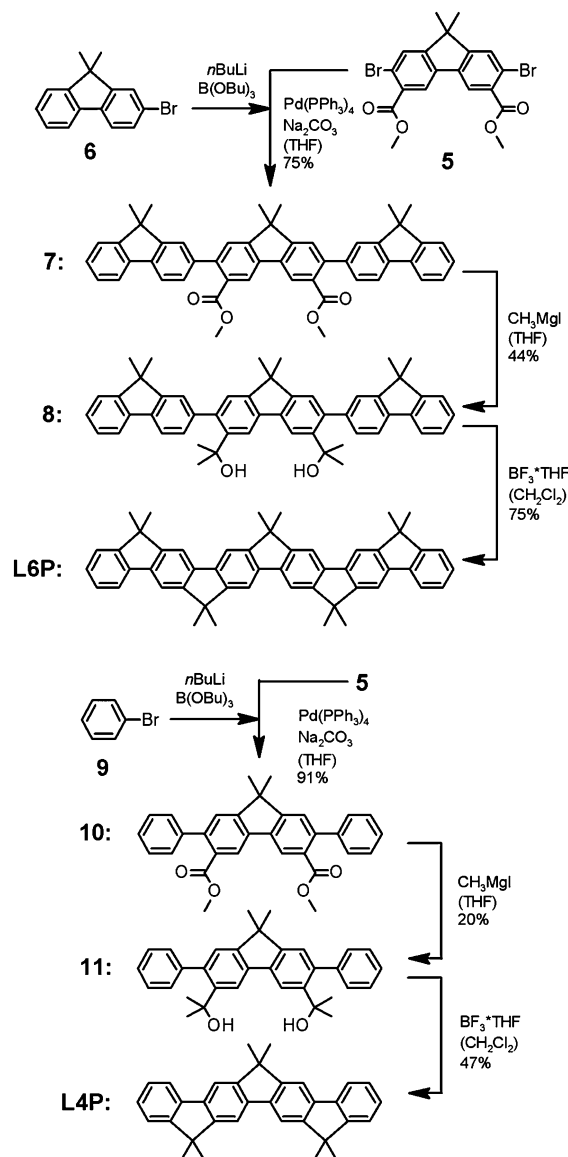
Our synthesis to even-numbered LOPPs is based on a central fluorene unit, which is connected to two terminal aromatic moieties *via* cross-coupling reactions. The bridging, leading to an extended aromatic system and hence extremely low solubility, represents the penultimate step of the sequence. The functional groups to induce the bridging reaction are incorporated in the central building block and hence access to the highly functionalized fluorene derivative **5** (Scheme 1) is required.

Since attempts to direct functionalization of 2,7-dimethylfluorene in its 3- and 6-position were not successful, phenanthrene-9,10-dione **1** was chosen as the starting material as it is regioselectively brominated using bromine and dibenzoyl peroxide in nitrobenzene.¹⁰ Ring contraction of 3,6-dibromophenanthrene-9,10-dione followed by decarboxylation using aqueous KOH and KMnO₄ provided 3,6-dibromofluorenone,¹¹ which was reduced *via* a Wolff–Kishner reduction¹² and the formed 3,6-dibromofluorene was subsequently methylated employing CH₃I and KO^{*t*}Bu¹³ to provide 3,6-dibromo-9,9-dimethylfluorene **2**.¹⁴ Two-fold lithiation using *n*-butyl lithium and subsequent reaction with chloromethyl methyl ether (MOM-Cl) gave **3** in 75% yield. Note that other electrophiles, such as dimethyl carbonate or acetone, gave lower yields. Diether **3** was brominated with *N*-bromosuccinimide in propylene carbonate¹⁵ and the formed 2,7-dibrominated fluorene **4** was oxidized¹⁶ to the corresponding diester building block **5**.

The core unit **5** was reacted with 9,9-dimethylfluorene-2-boronic acid, which was readily generated by lithiation of **6** followed by reaction with tributylborate (Scheme 2, top), in a Suzuki cross-coupling reaction employing catalytic amounts of Pd(PPh₃)₄ and Na₂CO₃ in a biphasic water–tetrahydrofuran (THF) solvent mixture.¹⁷ Diester **7** was treated with excess CH₃MgI to yield diol **8**. Final bridging *via* intramolecular Friedel–Crafts alkylation¹⁸ provides ladder-type sexiphenyl **L6P**, readily visible by its characteristic blue fluorescence appearing within a few seconds of the reaction. Purification of the final product **L6P** was achieved by precipitation, extensive washing of the solid, and final sublimation. Interestingly, the solubility of **L6P** in CHCl₃ and CH₂Cl₂ is much better as compared to *p*-sexiphenyl **6P** enabling characterization by standard solution techniques, such as NMR, UV/vis absorption and fluorescence measurement as well as cyclic voltammetry (CV). It appears that



Scheme 1 Synthesis of highly functionalized fluorene **5** (TEBAC = triethyl benzyl ammoniumchloride).



Scheme 2 Synthesis of ladder oligomers **L4P** and **L6P**.

the methyl groups at the sp³-hybridized bridging carbon atoms projecting out of plane prevent efficient π – π stacking, at least to some degree.

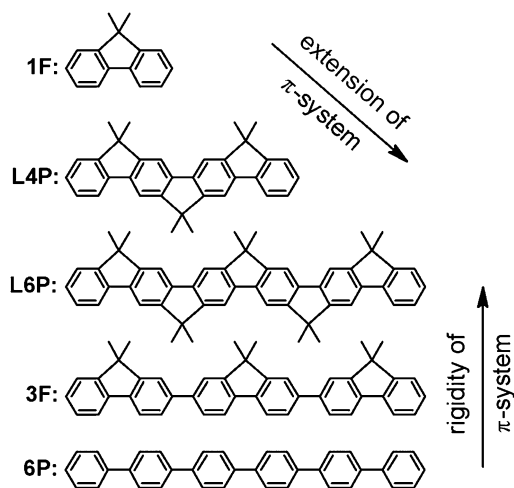
The synthesis of the ladder-type quarterphenyl **L4P** was carried out following an analogous route but employing phenylboronic acid (Scheme 2, bottom). Intermediate diester **10** was reacted with CH₃MgI to afford diol **11**, which was converted to **L4P** *via* two-fold intramolecular Friedel–Crafts alkylation. Purification of **L4P** was achieved by recrystallization and sublimation. For comparison purposes, bifluorene **2F**¹⁹ was synthesized by cross-coupling **6** with its corresponding boronic acid while terfluorene **3F** was synthesized according to literature procedures.²⁰

2.2 Optical and electrochemical properties

The optical and electrochemical behavior of the newly synthesized oligomers was investigated in solution, in particular to determine the influence of increasing rigidity, *i.e.* loss of rotational degrees of freedom, in a series ranging from **6P** over **3F** to

L6P as well as the effect of extending the π -system in even-numbered LOPPs in a series ranging from **1F** over **L4P** to **L6P** (Scheme 3).

Both absorption (λ_{abs}) and fluorescence emission (λ_{em}) maxima are bathochromically shifted with increasing degree of bridging, *i.e.* going from **6P** via **3F** to **L6P** (Fig. 1, top). This is in good agreement with the fact that bridging forces adjacent phenylene units into coplanarity hence leading to an increased effective π -conjugation. In addition, the maximum extinction coefficients ϵ_{max} are significantly increased upon bridging, *i.e.* it is more than doubled when going from **4P** to **L4P** and again from **3F** to **L6P** as well as more than tripled going from **6P** to **L6P** (Table 1). The absorption and excitation spectra of **3F** and **6P**,²¹ respectively, are rather broad and unstructured when compared to **L6P**. In addition to having a very high extinction coefficient ϵ_{max} the absorption maximum of **L6P** is very sharp, in particular on the low-energy edge. The degree of bridging has perhaps the most profound effect on the Stokes shift ($\Delta\bar{\nu}$), *i.e.* the energy offset between absorption and emission maxima, which is significantly decreased when going from **6P** (4700 cm^{-1}) via **3F** (2000 cm^{-1}) to **L6P** (300 cm^{-1} amounting to 0.04 eV only). These observations are readily explained by the fact that oligo(*p*-phenylene)s can freely rotate about the phenylene–phenylene bonds in the ground state in solution, leading to absorption of various rotamers and hence spectral broadening. Upon excitation the unbridged oligo (*p*-phenylene)s can undergo relaxation on their excited state potential energy surface by adopting a more planar conformation,²² hence giving rise to a large Stokes shift. In contrast, the geometry of the rigidified **L6P** in its ground and excited states is almost identical leading to a vanishing Stokes shift, while **3F** represents a somewhat intermediate case. Furthermore, rigidification in **L6P** is reflected by the clearly visible vibronic coupling. In this regard, analysis of the absorption spectra of the bridged series, *i.e.* **1F**, **L4P**, and **L6P** (Fig. 1, bottom), shows that in all cases the 0,0-transition is favored. The distance between the 0,0- and 0,1-transitions varies between 1250 and 1450 cm^{-1} . Importantly, the fluorescence quantum yield (Φ) of both **L6P** and **3F** is close to unity.²³ With increasing size of the π -system, the quantum yields seem to increase only slightly (Table 1).



Scheme 3 Characterized compounds and variation of their structural parameters.

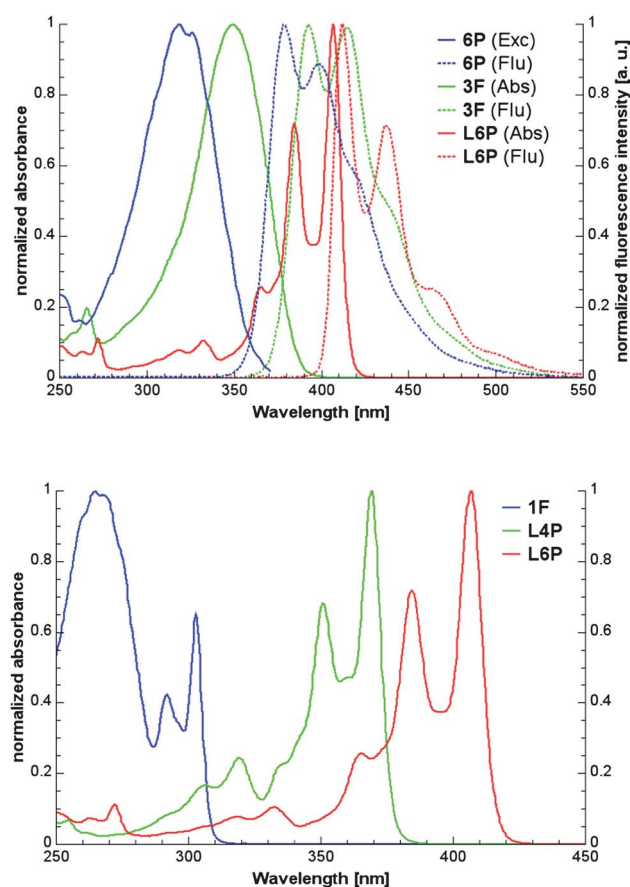


Fig. 1 Spectral properties of *p*-phenylenes in solution: absorption (Abs), excitation (Exc), and fluorescence (Flu) spectra of **6P**, **3F**, and **L6P** in CH_2Cl_2 (top). Absorption spectra of **1F**, **L4P**, and **L6P** in CH_2Cl_2 (bottom).

In addition to the optical properties, the electrochemical behavior of the newly synthesized LOPPs has been investigated and compared to their respective compounds. The cyclic voltammograms of **3F** (Fig. 2, top) and **L6P** (Fig. 2, bottom) show that both compounds can reversibly be oxidized in two successive one-electron steps to their respective radical cations and dication. The bridged structure in **L6P** facilitates the first oxidation event, as it occurs at a 300 mV lower oxidation potential as compared to **3F** (Table 2). Furthermore, the enhanced π -conjugation and therefore stronger coupling lead to

Table 1 Optical properties of the investigated *p*-phenylenes in solution^a

	$\lambda_{\text{abs}}/\text{nm}$	$\epsilon_{\text{max}}/\text{M}^{-1} \text{cm}^{-1}$	$\lambda_{\text{em}}/\text{nm}$	Φ	$\Delta\bar{\nu}/\text{cm}^{-1}$
6P	320 ^b	55 000 ^c	377	0.93 ^c	4700
3F	349	90 000	393	0.99	2000
L6P	407	190 000	412	0.92	300
L4P	369	100 000	374	0.67	360
1F	301	16 000	303	0.53–0.80 ^d	220
4P ^e	295	41 000		0.89	

^a In CH_2Cl_2 at 25 °C. ^b Maximum of excitation spectrum. ^c Values according to ref. 24. ^d Values for non-methylated fluorene according to ref. 25 and 26. ^e Values according to ref. 27.

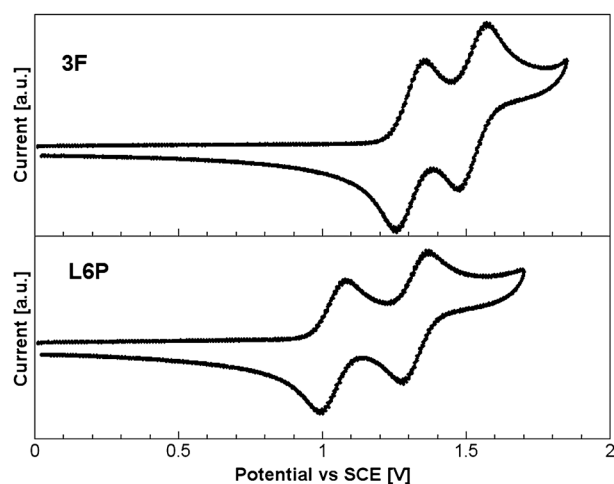


Fig. 2 Cyclic voltammogram of **3F** (top) and **L6P** (bottom) in CH_2Cl_2 (0.1 M Bu_4NPF_6), $dE/dt = 1 \text{ V s}^{-1}$.

a greater separation of the two oxidation peaks (ΔE_p^a) in **L6P** (Table 2). The same trends are observed when comparing **2F** with its bridged analogue **L4P**. Therefore, the completely bridged structures become more electron-rich, which could in part be attributed to their smaller HOMO–LUMO gap, and their radical cations are more stabilized by the enhanced π -conjugation as compared to their dications. Furthermore, the number of reversible one-electron oxidation steps of LOPPs as a function of the number of phenylene units is basically the same as reported for oligo(*p*-fluorene)s.^{28,29} Thus, whereas the oxidation of **1F** is irreversible, **L4P** forms a stable radical cation yet undergoes an irreversible second electron transfer, and **L6P** exhibits two reversible oxidation steps.

While performing the cyclic voltammetric measurements with **L6P** UV/vis absorption spectra were recorded (Fig. 3). The formation of the radical cation **L6P^{•+}** is indicated by a newly formed absorption band maximum located at 581 nm. Moving to higher potential the absorption band of the dication **L6P²⁺** can be observed with a maximum at 1084 nm. Note that the spectral shape of the three species remains rather similar as all three compounds display three maxima, due to vibronic transitions, and the distance between the first and second absorption maximum remains at about 1450–1500 cm^{-1} .

2.3 Thin film growth

Initial studies were carried out by evaporating **L6P** onto quartz slides using a conventional sublimation apparatus and

Table 2 Oxidation potentials of investigated *p*-phenylenes^a

	E_p^{a1}/V	E_p^{a2}/V	$\Delta E_p^a/\text{V}$
3F	0.793	1.009	0.216
L6P	0.492	0.778	0.286
L4P	0.687	1.193 ^b	0.506
1F	1.276 ^b	—	—
2F	0.894	1.248 ^b	0.354

^a Potentials vs. Fc/Fc^+ in CH_2Cl_2 (0.1 M Bu_4NPF_6), $dE/dt = 1 \text{ V s}^{-1}$.

^b Irreversible oxidation.

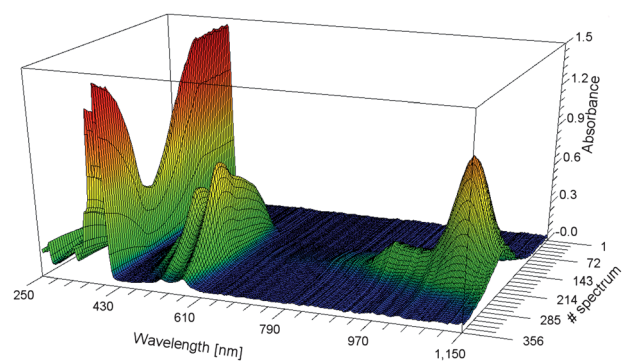


Fig. 3 Spectral change of **L6P** during electrochemical oxidation: formation of radical cation and dication ($c = 8 \times 10^{-5} \text{ M}^{-1}$ in CH_2Cl_2). Recorded in a 1 mm quartz cuvette using a platinum grid electrode, 0.1 M Bu_4NPF_6 , $dE/dt = 10 \text{ mV s}^{-1}$, $0 \rightarrow 1.3 \rightarrow 0 \text{ V vs. Ag}/\text{AgNO}_3$, spectra recorded every 7.3 mV.

comparing the resulting films with drop-cast films (of varying thickness). Inspection of the optical absorption and emission spectra of **L6P** (Fig. 4) shows the characteristic features already discussed for the corresponding solution spectra (see Fig. 1). Regardless of the method for film formation, the spectral shapes are rather similar reproducing all absorption and emission maxima. However, it appears that in the case of the vacuum-deposited film some bands in the absorption spectrum are more pronounced, in particular the maximum at *ca.* 350 nm, while the long-wavelength edge of the emission is significantly broadened. We attribute these changes to higher degree of crystallinity in the vacuum-deposited samples as compared to the ones cast from solution. This is further supported by AFM measurements (see below). Importantly, these initial results suggest that the ladder oligomer **L6P** can successively be vacuum-deposited without undergoing thermal decomposition.

Thin films of **L6P** were prepared on Al_2O_3 (0001) substrates by OMBD in an UHV (5×10^{-9} Torr) deposition chamber. The deposition rate as measured by a quartz microbalance was 0.1 nm min^{-1} . The substrate was kept at room temperature. The morphology of a **L6P** submonolayer at a coverage of 0.27 is depicted in the AFM image of Fig. 5. Extended flat molecular

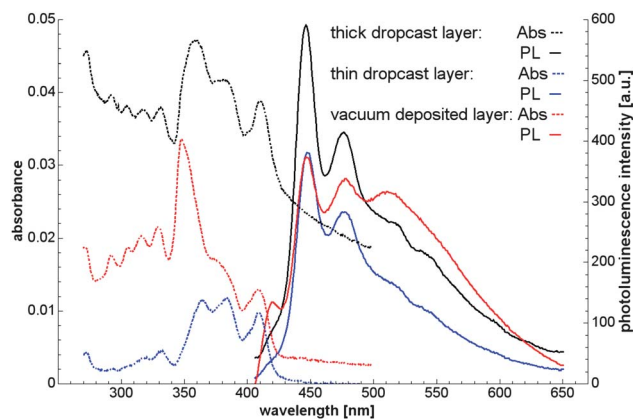


Fig. 4 Absorption (Abs) and photoluminescence (PL) spectra of thin films of **L6P** on quartz substrates, either prepared by vacuum deposition or drop-casting from CH_2Cl_2 solution.

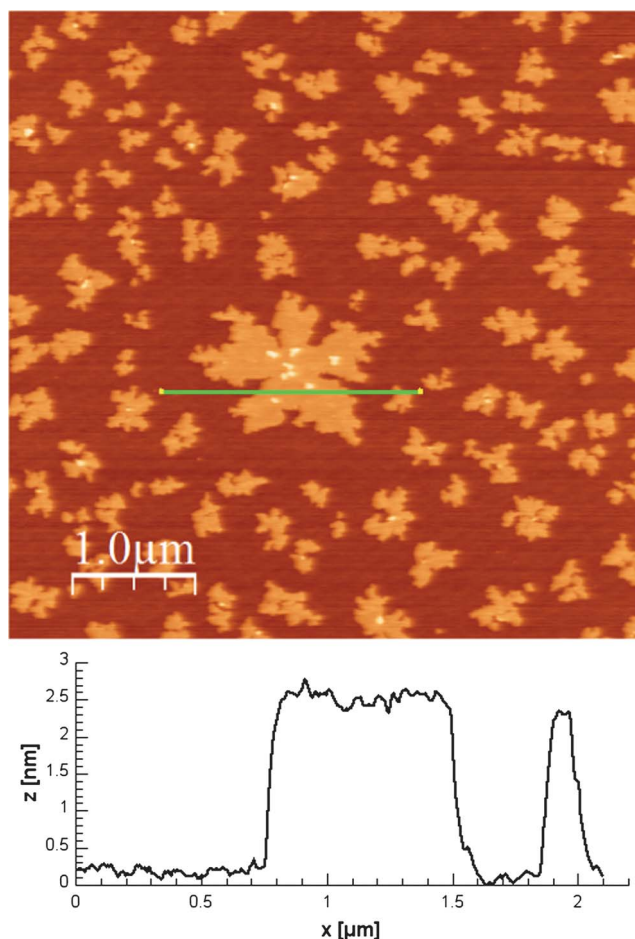


Fig. 5 AFM image of **L6P** deposited on an Al_2O_3 (0001) surface (top) and the corresponding height profile (bottom).

islands with a height corresponding approximately to the length of the **L6P** are visible. Thus, the islands are comprised of upright standing molecules. Such morphology is typical for molecules crystallizing in a herringbone structure on chemically inert substrates (such as sapphire). It was found also for **6P** molecules deposited on ZnO (0001)² and TiO_2 .³⁰

3. Conclusions

A new synthetic route to yield even-numbered LOPPs has been developed based on the use of a highly functionalized central fluorene building block. Direct comparison with the structurally related non-bridged oligo(*p*-phenylene)s as well as partially bridged oligofluorenes shows that the newly synthesized LOPPs exhibit outstanding photophysical properties, such as sharp and intense optical transitions characterized by narrow absorption bands and very small Stokes shifts as well as large extinction coefficients and high fluorescence quantum yields. The origin of the observed optical properties can clearly be linked to their rigid structure maximizing π -conjugation. Furthermore, oxidation of LOPPs is more facile as compared to their non-bridged counterparts. Initial investigations demonstrate that these materials are applicable to OMBD techniques allowing the controlled generation of organic (ultra)thin films on solid substrate surfaces. In conjunction with inorganic

semiconductors, such hybrid inorganic–organic structures, merging the advantageous properties of both material classes promise exciting new phenomena to be unraveled and exploited for optoelectronic and photonic applications.

4. Experimental section

Absorption measurements were carried out on a Varian Cary 50 Bio UV/vis spectrometer in 1 cm quartz cuvettes. Fluorescence spectra were obtained on a Varian Cary Eclipse spectrofluorimeter. Solutions of a concentration of about 10^{-6} mol L^{-1} (for dimethylfluorene about 10^{-5} mol L^{-1}) were used for the absorption measurements. Perylene ($\Phi = 94\%$, ref. 25) was used as references for the measurement of the fluorescence quantum yields. It was dissolved in cyclohexane, the other products in CH_2Cl_2 . The solutions were diluted 1 by 30 for the measurement of fluorescence spectra. The reference solution was degassed with argon before carrying out the measurements. Electrochemical measurements were carried out using a HEKA-Elektronik PG310 potentiostat or an Autolab PGSTAT128N and an Ava Spec-2048x14 spectrometer equipped with an Avalight-DH-S-BAL lamp. $^1\text{H-NMR}$ and $^{13}\text{C-NMR}$ spectra were referenced to 7.26 ppm and 77.16 ppm, respectively, for CDCl_3 and 5.32 ppm and 53.8 ppm, respectively, for CD_2Cl_2 . Thin films of **L6P** were grown in an OMBD system by CreaPhys. The AFM image was recorded in tapping mode with a Nanoscope 3a controller, Veeco, USA.

3,6-Dibromophenanthrene-9,10-dione

The literature procedure¹⁰ was adapted to large scale synthesis: phenanthrene-9,10-dione **1** (52 g, 250 mmol) and dibenzoyl peroxide (2 g, 8.3 mmol) were dissolved in nitrobenzene (250 mL). An initial amount of bromine (14.5 g, 90 mmol) was added to the mixture and heated to 120 °C. When the formation of gaseous HBr started, the remaining bromine (72 g, 450 mmol, in sum 86.4 g, 540 mmol) was added dropwise. After heating for one hour, the mixture was cooled and ethanol (250 mL) was added. The precipitated product was filtered and washed with ethanol until the washing solution turned colourless. After drying under vacuum 83.4 g (228 mmol, 91% yield) 3,6-dibromophenanthrene-9,10-dione were obtained as an orange powder. $^1\text{H-NMR}$ (500 MHz, CDCl_3) δ (ppm) 8.12 (d, $J = 1.8$ Hz, 2H), 8.07 (d, $J = 8.3$ Hz, 2H), 7.67 (dd, $J = 8.3, 1.7$ Hz, 2H). $^{13}\text{C-NMR}$ (126 MHz, CDCl_3) δ (ppm) 179.0, 136.1, 133.6, 132.3, 130.0, 127.6.

3,6-Dibromo-9-fluorenone

The literature procedure¹¹ was used: KOH (101 g, 2.2 mol) was dissolved in 150 mL of water and heated to 130 °C. Then, 3,6-dibromophenanthrene-9,10-dione (61.9 g, 169 mmol) was suspended in the solution. After stirring for 30 min, the mixture turned black and very viscous. Within a period of 2 h KMnO_4 (141.5 g, 895 mmol) was added carefully. The mixture was stirred at 130 °C for one hour and cooled to room temperature, followed by neutralization with concentrated sulfuric acid. Sodium bisulfite was added carefully to the (slightly acidic!) mixture until it turned light yellow. The precipitate was filtered off and washed with water. 3,6-Dibromo-9-fluorenone (41.1 g, 121.6 mmol, 72% yield) was obtained as a light yellow powder. $^1\text{H-NMR}$ (500

MHz, CDCl₃) δ (ppm) 7.67 (d, J = 1.6 Hz, 2H), 7.55 (d, J = 7.8 Hz, 2H), 7.50 (dd, J = 7.8, 1.6 Hz, 2H).

3,6-Dibromofluorene

The literature procedure¹² was modified concerning workup and purification: 3,6-dibromo-9-fluorenone (33.8 g, 100 mmol) was dispersed in 300 mL of triethylene glycol and hydrazine hydrate (100%, 21.8 mL, 450 mmol) was added. While stirring overnight at 100 °C the solution slowly turned clear. Then, KOH (33 g in 90 mL of water) was added. Stirring was continued for 2 h at 130 °C. After cooling to room temperature, the mixture was poured into 1.2 L of water and neutralized with HCl. The orange precipitate was filtered off, dried and purified by sublimation (10⁻³ mbar, heater at 220 °C). 3,6-Dibromofluorene (20.2 g, 62.3 mmol, 62% yield) was obtained as a nearly white solid. ¹H-NMR (500 MHz, CDCl₃) δ (ppm) 7.87 (d, J = 1.7 Hz, 2H), 7.44 (dd, J = 8.0, 1.8 Hz, 2H), 7.40 (d, J = 8.0 Hz, 2H), 3.80 (s, 2H). ¹³C-NMR (126 MHz, CDCl₃) δ (ppm) 142.8, 142.3, 130.4, 126.7, 123.5, 121.2, 36.4.

3,6-Dibromo-9,9-dimethylfluorene (2)

The literature procedure¹³ was adapted to the substrate: 3,6-dibromofluorene (17.8 g, 55 mmol) was dissolved in dry THF (150 mL) and cooled to 0 °C. KO^tBu (18.5 g, 165 mmol), and after stirring for 10 min, CH₃I (10.3 mL, 165 mmol) were added. The solution was allowed to warm to room temperature and it was stirred overnight. Then water was added and the mixture was extracted with ethyl acetate. The organic phase was dried with MgSO₄. Upon removing the solvent, the crude product remained as an orange solid. Column chromatography (cyclohexane) gave 12.2 g (34.7 mmol, 63% yield) 3,6-dibromo-9,9-dimethylfluorene **2** as a white solid. ¹H-NMR (500 MHz, CDCl₃) δ (ppm) 7.80 (d, J = 1.8 Hz, 2H), 7.45 (dd, J = 8.0, 1.8 Hz, 2H), 7.29 (d, J = 8.0 Hz, 2H), 1.45 (s, 6H). ¹³C-NMR (126 MHz, CDCl₃) δ (ppm) 152.7, 140.2, 130.9, 124.4, 123.6, 121.2, 46.8, 26.9.

3,6-Bis(methoxymethyl)-9,9-dimethylfluorene (3)

3,6-Dibromo-9,9-dimethylfluorene **2** (12 g, 34 mmol) was dissolved under argon in 200 mL of dry THF and the solution was cooled to -78 °C. *n*-BuLi (2.2 M in cyclohexane, 42 mL, 92 mmol) was added and the solution was stirred for 30 min. Then, chloromethyl methyl ether (MOM-Cl, 8.5 mL, 112 mmol) was added and stirring was continued for 30 min at -78 °C and overnight (solution turned clear after 10 min) at room temperature. The mixture was poured into water. It was extracted with ethyl acetate, dried (MgSO₄) and the solvent was removed. Column chromatography (petroleum ether (b.p. 40–60 °C)/ethyl acetate) gave 7.2 g (25.5 mmol, 75% yield) 3,6-bis(methoxymethyl)-9,9-dimethylfluorene **3**. ¹H-NMR (500 MHz, CDCl₃) δ (ppm) 7.73 (d, J = 0.7 Hz, 2H), 7.41 (d, J = 7.7 Hz, 2H), 7.29 (dd, J = 7.7, 1.3 Hz, 2H), 4.54 (s, 4H), 3.44 (s, 6H), 1.48 (s, 6H). ¹³C-NMR (126 MHz, CDCl₃) δ (ppm) 153.6, 139.5, 137.2, 127.1, 122.6, 119.7, 95.8, 75.1, 58.3, 46.7, 27.3.

2,7-Dibromo-3,6-bis(methoxymethyl)-9,9-dimethylfluorene (4)

The literature procedure¹⁵ was adapted to substrate **3**: in 30 mL of propylene carbonate 3,6-bis(methoxymethyl)-9,9-

dimethylfluorene **3** (1.9 g, 6.7 mmol) was dissolved and NBS (2.4 g, 13.4 mmol) was added. The mixture was stirred for 16 h at 60 °C. Then, water was added and the precipitate was filtered off. Purification by column chromatography gave 2.5 g (5.7 mmol, 85% yield) 2,7-dibromo-3,6-bis(methoxymethyl)-9,9-dimethylfluorene **4** as a colorless solid. ¹H-NMR (500 MHz, CDCl₃) δ (ppm) 7.82 (s, 2H), 7.57 (s, 2H), 4.59 (s, 4H), 3.53 (s, 6H), 1.46 (s, 6H). ¹³C-NMR (126 MHz, CDCl₃) δ (ppm) 154.4, 138.0, 136.6, 127.1, 121.8, 120.7, 74.3, 58.9, 47.1, 27.1.

Dimethyl-2,7-dibromo-9,9-dimethylfluorene-3,6-dicarboxylate (5)

The literature procedure¹⁶ was adapted to substrate **4**: in 10 mL of CH₂Cl₂ 2,7-dibromo-3,6-bis(methoxymethyl)-9,9-dimethylfluorene **4** (0.16 g, 0.36 mmol), benzyltriammonium chloride (TEBAC, 0.49 g, 2.16 mmol) and KMnO₄ (0.34 g, 2.16 mmol) were dissolved and stirred for 5 h at reflux. Then an aqueous solution of sodium thiosulfate was added until the purple color disappeared. The mixture was extracted with CH₂Cl₂, dried (MgSO₄) and the solvent was removed. Column chromatography (cyclohexane/ethyl acetate) gave 0.15 g (0.32 mmol, 89% yield) dimethyl 2,7-dibromo-9,9-dimethylfluorene-3,6-dicarboxylate **5**. ¹H-NMR (500 MHz, CDCl₃) δ (ppm) 8.13 (s, 2H), 7.69 (s, 2H), 3.97 (s, 6H), 1.48 (s, 6H). ¹³C-NMR (126 MHz, CDCl₃) δ (ppm) 166.7, 157.7, 136.9, 131.4, 129.2, 123.3, 121.5, 52.7, 47.8, 26.6.

2-Bromo-9,9-dimethylfluorene (6)

2-Bromofluorene (10 g, 40.8 mmol) was dissolved in 200 mL of DMSO and cooled to 0 °C. Then, CH₃I (6.1 mL, 97.9 mmol), TEBAC (0.46 g, 2 mmol) and 25 mL of 50% aq. NaOH were added. After stirring for 30 min, the solution was poured into water and extracted with ethyl acetate. The organic phase was washed with HCl, dried with MgSO₄ and the solvent was removed. Column chromatography (petroleum ether/ethyl acetate) gave 11 g (40.2 mmol, 99% yield) 2-bromo-9,9-dimethylfluorene **6**. ¹H-NMR (300 MHz, CDCl₃) δ (ppm): 7.73–7.68 (m, 1H), 7.61–7.57 (m, 2H), 7.50–7.42 (m, 2H), 7.38–7.33 (m, 2H), 1.49 (s, 6H). ¹³C-NMR (75 MHz, CDCl₃) δ (ppm) 155.8, 153.4, 138.3, 138.2, 130.2, 127.8, 127.3, 126.2, 122.8, 121.5, 121.1, 120.2, 47.2, 27.1.

Terfluorene (7)

General procedure for Suzuki coupling according to ref. 17: 2-bromo-9,9-dimethylfluorene **6** (4.8 g 17.5 mmol) was dissolved under argon atmosphere in 50 mL of dry THF and cooled to -78 °C. Subsequently *n*-BuLi (2.2 M in cyclohexane, 8.9 mL, 19.6 mmol) was added and the mixture was stirred for 30 min. It turned brown and milky. Upon adding tributylborate (5.7 mL, 21 mmol), the solution was stirred for one hour at room temperature.

Meanwhile dimethyl 2,7-dibromo-9,9-dimethylfluorene-3,6-dicarboxylate **5** (3.3 g, 7 mmol) was dissolved in 50 mL of THF and degassed using argon. Then, Pd(PPh₃)₄ (0.65 g, 0.56 mmol) was added. After stirring for 15 min, 40 mL of 2 M aq. sodium carbonate solution was added and the temperature was raised to 60 °C.

Both solutions were combined and stirred overnight at 60 °C. After cooling to room temperature, water was added and the mixture was extracted with ethyl acetate. The organic phase was dried (MgSO₄) and the solvent was removed. The crude product was first purified by column chromatography and then dissolved in a mixture of CH₂Cl₂ and ethyl acetate. CH₂Cl₂ was removed under reduced pressure and the product precipitated. Upon suction and drying under vacuum 3.6 g (5.2 mmol, 74% yield) of terfluorene **7** were obtained. ¹H-NMR (500 MHz, CDCl₃) δ (ppm) 8.26 (s, 2H), 7.81 (d, *J* = 8.1 Hz, 2H), 7.80–7.77 (m, 2H), 7.56 (s, 2H), 7.50–7.46 (m, 2H), 7.46–7.42 (m, 4H), 7.41–7.33 (m, 4H), 3.67 (s, 6H), 1.61 (s, 6H), 1.56 (s, 12H). ¹³C-NMR (126 MHz, CDCl₃) δ (ppm) 169.9, 156.9, 153.9, 153.7, 142.5, 140.8, 139.0, 138.6, 137.4, 130.9, 127.5, 127.4, 127.2, 125.1, 123.0, 122.8, 122.0, 120.3, 120.0, 52.2, 47.8, 47.0, 27.4, 27.1.

Dimethyl 2,7-diphenyl-9,9-dimethylfluorene-3,6-dicarboxylate (10)

Starting from bromobenzene **9** (0.47 g, 3 mmol) and dimethyl 2,7-dibromo-9,9-dimethylfluorene-3,6-dicarboxylate **5** (0.47 g, 1 mmol), 0.42 g (0.91 mmol, 91% yield) dimethyl 2,7-diphenyl-9,9-dimethylfluorene-3,6-dicarboxylate **10** was obtained without the above mentioned crystallization step. ¹H-NMR (500 MHz, CDCl₃) δ (ppm) 8.24 (s, 2H), 7.47–7.42 (m, 6H), 7.41–7.37 (m, 6H), 3.69 (s, 6H), 1.54 (s, 6H). ¹³C-NMR (126 MHz, CDCl₃) δ (ppm) 169.2, 156.8, 142.5, 141.7, 137.3, 130.3, 128.4, 128.1, 127.3, 125.2, 121.9, 52.0, 47.6, 26.9.

Terfluorene diol (8)

General procedure for the reaction of terfluorene diesters with Grignard reagents to terfluorene diols: terfluorene **7** (0.9 g, 1.3 mmol) was dissolved in 50 mL of dry THF under argon and CH₃MgI (3 M in diethyl ether, 10.8 mL, 32.5 mmol) was added. After refluxing for 2 h, water was added and the mixture was extracted with diethyl ether. The organic phase was dried with MgSO₄ and the solvent was removed. Column chromatography (cyclohexane/ethyl acetate) gave 0.40 g (0.58 mmol, 44% yield) of terfluorene **8**. ¹H-NMR (500 MHz, CD₂Cl₂) δ (ppm) 8.16 (s, 2H), 7.80–7.76 (m, 4H), 7.51–7.46 (m, 4H), 7.36 (m, 6H), 7.21 (s, 2H), 2.12 (s, 2H), 1.53 (s, 12H), 1.52 (s, 12H), 1.49 (s, 6H). ¹³C-NMR (75 MHz, CD₂Cl₂) δ (ppm) 154.2, 153.5, 152.0, 146.3, 143.7, 140.0, 139.2, 138.6, 138.3, 129.0, 127.7, 127.4, 126.6, 124.8, 123.0, 120.3, 119.5, 117.8, 74.4, 47.2, 46.8, 33.0, 27.4, 27.2.

2,7-Diphenyl-3,6-bis(1,1-dimethylhydroxymethyl)-9,9-dimethylfluorene (11)

Starting from dimethyl 2,7-diphenyl-9,9-dimethylfluorene-3,6-dicarboxylate **10** (0.4 g, 0.87 mmol), 0.08 g (0.17 mmol, 20% yield) 2,7-diphenyl-3,6-bis(1,1-dimethylhydroxymethyl)-9,9-dimethylfluorene **11** was obtained. ¹H-NMR (500 MHz, CD₂Cl₂) δ (ppm) 8.10 (s, 2H), 7.43–7.36 (m, 10H), 7.10 (s, 2H), 1.82 (s, 2H), 1.51 (s, 12H), 1.43 (s, 6H).

Ladder-type sexiphenyl (L6P)

General procedure for the intramolecular Friedel–Crafts reaction to ladder-type *p*-phenylenes according to ref. 18: terfluorene

8 (0.4 g, 0.57 mmol) was dissolved in 50 mL of CH₂Cl₂ and BF₃·THF (50% in THF, 1.9 mL, 8.5 mmol) was added. After stirring for 30 min at room temperature, ethanol and aq. NaHCO₃ were added. The organic phase was concentrated and the product was separated by centrifugation. The yellowish precipitate was washed with ethyl acetate several times. Finally, 0.28 g (0.42 mmol, 75% yield) of the ladder-type sexiphenyl **L6P** was obtained. ¹H-NMR (500 MHz, CDCl₃) δ (ppm) 7.84 (s, 6H), 7.80–7.77 (m, 4H), 7.46 (d, *J* = 7.3 Hz, 2H), 7.36 (td, *J* = 7.4, 0.9 Hz, 2H), 7.31 (td, *J* = 7.2, 0.9 Hz, 2H), 1.66 (s, 6H), 1.65 (s, 12H), 1.59 (s, 12H). ¹³C-NMR (126 MHz, CDCl₃) δ (ppm) 154.2, 153.8, 153.8, 153.7, 153.3, 139.7, 139.3, 139.0, 138.9, 138.6, 127.1, 127.0, 122.7, 119.8, 114.3, 114.0, 114.0, 113.9, 46.7, 46.5, 29.9, 27.9, 27.6.

Ladder-type quarterphenyl (L4P)

Starting with 2,7-diphenyl-3,6-bis(1,1-dimethylhydroxymethyl)-9,9-dimethylfluorene **11** (0.07 g, 0.15 mmol), 0.03 g (0.07 mmol, 47% yield) of the ladder-type quarterphenyl **L4P** was obtained after recrystallization from ethyl acetate. ¹H-NMR (500 MHz, CDCl₃) δ (ppm) 7.83 (s, 2H), 7.79–7.76 (m, 4H), 7.46 (d, *J* = 7.2 Hz, 2H), 7.36 (td, *J* = 7.4, 1.2 Hz, 2H), 7.31 (td, *J* = 7.3, 1.1 Hz, 2H), 1.62 (s, 6H), 1.58 (s, 12H). ¹³C-NMR (75 MHz, CDCl₃) δ (ppm) 154.0, 153.6, 153.1, 139.5, 139.0, 138.5, 127.0, 126.9, 122.6, 119.7, 114.2, 113.9, 46.6, 46.3, 27.7, 27.4.

Acknowledgements

Generous support by the German Research Foundation (DFG via SFB 951) is gratefully acknowledged. Wacker Chemie AG, BASF AG, Bayer Industry Services, and Sasol Germany are thanked for generous donations of chemicals.

References

- 1 S. K. So, *Organic Electronics*, CRC Press, Boca Raton, 2010.
- 2 S. Blumstengel, H. Glowatzki, S. Sadofev, N. Koch, S. Kowarik, J. P. Rabe and F. Henneberger, *Phys. Chem. Chem. Phys.*, 2010, **12**, 11642.
- 3 S. Forrest, *Chem. Rev.*, 1997, **97**, 1793–1896.
- 4 G. Leising, F. Meghdadi, S. Tasch, C. Brandstätter, W. Graupner and G. Kranzelbinder, *Synth. Met.*, 1997, **85**, 1209.
- 5 Y. Ohmori, T. Tsukagawa and H. Kajii, *Displays*, 2001, **22**, 61.
- 6 R. Resel, *J. Phys.: Condens. Matter*, 2008, **20**, 184009.
- 7 S. Blumstengel, S. Sadofev, C. Xu, J. Puls, R. L. Johnson, H. Glowatzki, N. Koch and F. Henneberger, *Phys. Rev. B: Condens. Matter Mater. Phys.*, 2008, **77**, 085323.
- 8 Reviews are given in (a) A. C. Grimsdale and K. Müllen, *Macromol. Rapid Commun.*, 2007, **28**, 1676; (b) A. C. Grimsdale and K. Müllen, *Adv. Polym. Sci.*, 2008, **212**, 1 Some selected examples include (c) J. Grimme, M. Kreyenschmidt, F. Uckert, K. Müllen and U. Scherf, *Adv. Mater.*, 1995, **7**, 292; (d) J. Grimme and U. Scherf, *Macromol. Chem. Phys.*, 1996, **197**, 2297; (e) F. Schindler, J. Jacob, A. C. Grimsdale, U. Scherf, K. Müllen, J. M. Lupton and J. Feldmann, *Angew. Chem., Int. Ed.*, 2005, **44**, 1520; (f) N. Cocherel, C. Poriel, J. Rault-Berthelot, F. Barriere, N. Audebrand, A. M. Z. Slawin and L. Vignau, *Chem.–Eur. J.*, 2008, **14**, 11328; (g) Q. Zheng, S. K. Gupta, G. S. He, L.-S. Tan and P. N. Prasad, *Adv. Funct. Mater.*, 2008, **18**, 2770; (h) H. Usta, C. Risko, Z. Wang, H. Huang, M. K. Deliomerglu, A. Zhukhovitskiy, A. Facchetti and T. J. Marks, *J. Am. Chem. Soc.*, 2009, **131**, 5586; (i) Q. Zheng, B. J. Jung, J. Sun and H. E. Katz, *J. Am. Chem. Soc.*, 2010, **132**, 5394.

-
- 9 The only exception known to us is a patent: EP 1860097 A1, *Aromatic Amine Derivative and Electroluminescence Device Utilizing the same*, M. Kimura, C. Hosokawa and M. Funahashi.
- 10 K. Brunner, A. van Dijken, H. Börner, J. J. A. M. Bastiaansen, N. M. M. Kiggen and B. M. W. Langeveld, *J. Am. Chem. Soc.*, 2004, **126**, 6035.
- 11 J. Ipaktschi, R. Hosseinzadeh, P. Schlaf and E. Dreiseidler, *Helv. Chim. Acta*, 1998, **81**, 1821.
- 12 Y. Song, W. Xu and D. Zhu, *Tetrahedron Lett.*, 2010, **51**, 4894.
- 13 C.-S. Li, Y.-H. Tsai, W.-C. Lee and W.-J. Kuo, *J. Org. Chem.*, 2010, **75**, 4004.
- 14 See also patent: US 2009/0030202 A1: *Material for Organic Electroluminescent Element and Element employing the same*, T. Iwakuma, *et al.*
- 15 S. Kajigaeshi, T. Kadowaki, A. Nishida and S. Fujisaki, *Bull. Chem. Soc. Jpn.*, 1986, **59**, 97.
- 16 J. H. Markgraf and B. Y. Choi, *Synth. Commun.*, 1999, **29**, 2405.
- 17 L. Lucas, J. J. D. de Jong, J. H. van Esch, R. M. Kellogg and B. L. Feringa, *Eur. J. Org. Chem.*, 2003, 155.
- 18 U. Scherf and K. Müllen, *Synthesis*, 1992, 23.
- 19 See also patent: WO 2004/020387 A1: *Monoaminofluorene Compound and Organic Light-emitting Device using the same*.
- 20 L. Lafferentz, F. Ample, H. Yu, S. Hecht, C. Joachim and L. Grill, *Science*, 2009, **323**, 1193.
- 21 For **6P** only excitation spectra are available due to its poor solubility.
- 22 J. R. Lakowicz, *Principles of Fluorescence Spectroscopy*, Kluwer, 2nd edn, 1999.
- 23 Due to its low solubility, no fluorescence quantum yield could be determined for **6P** by the employed method (ref. 22).
- 24 N. I. Nijgorodov, W. S. Downey and M. B. Danailo, *Spectrochim. Acta, Part A*, 2000, **56**, 783.
- 25 J. B. Birks, *Photophysics of Aromatic Molecules*, Wiley, London, 1970.
- 26 G. G. Guilbault, *Practical Fluorescence*, Marcel Dekker, New York, 1973.
- 27 I. B. Berlman, *Handbook of Fluorescence Spectra of Aromatic Molecules*, Academic Press, 1971.
- 28 C. Chi and G. Wegner, *Macromol. Rapid Commun.*, 2005, **26**, 1532.
- 29 J. Rault-Berthelot and J. Simonet, *J. Electroanal. Chem.*, 1985, **182**, 187.
- 30 R. Resel, M. Oehzelt, O. Lengyel, T. Haber, T. Schüllli, A. Thierry, G. Hlawacek, C. Teichert, S. Berkebile, G. Koller and M. Ramsey, *Surf. Sci.*, 2006, **600**, 4645.